로터 후류 효과를 고려한 헬리콥터 동체의 착빙 형상 예측

ICE ACCRETION ON A HELICOPTER FUSELAGE CONSIDERING THE ROTOR WAKE EFFECTS

손찬규 *, 오세종
부산대학교 항공우주공학과

이관중
서울대학교 기계항공공학부

CONTENTS

Motivation

Helicopter icing

- Operating helicopters in icing conditions is particularly dangerous
- Blade icing
  - ✓ Rotor blades are especially susceptible to ice growth due to their short chord length
  - ✓ Quick accumulating ice on the rotor systems leads to increased vibration, rapid loss of lift and a large power increase to sustain flight
  - ✓ Shed ice from spinning rotor is common and creates dangerous projectiles
- Fuselage icing : considering relatively unimportant parts
  - ✓ Windshield icing will obstruct the pilot's field of view, making landing and hovering operations difficult
  - ✓ Icing on the nacelle and engine intakes can result in engine failure
  - ✓ Icing on the sensory equipment, antenna, and masts can cause impaired data acquisition
  - ✓ Fuselage icing increases parasite drag, mass, and fuel consumption
- Problems to numerical approaches
  - ✓ Flowfield analysis from rotor is essential
  - ✓ 3D effect is dominant contrast to blade with high aspect ratio

▲ Front left of Puma with ice accretion

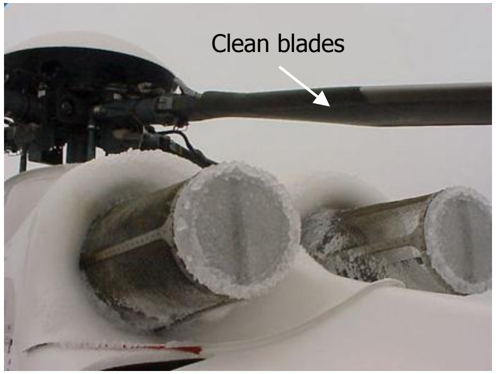

▲ Air intakes iced-up with clean blades

▲ Ice build-up on the mirrors of Puma

Motivation

Previous studies

- BELL 412 Helicopter(Szilder, K. 2007, 2010*)
  - ✓ With rotor and without rotor
  - ✓ Aerodynamic solver : Euler equation
  - ✓ Impingement model : Lagrangian approach
  - ✓ Thermodynamic model : not used, only rime ice condition

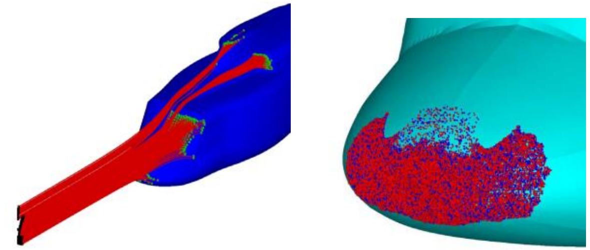

▲ Droplet trajectories and ice shapes on the fuselage nose*

- ROBIN body(Fouladi, H. 2013**)
  - ✓ With rotor and without rotor
  - ✓ Aerodynamic solver : Dree's inflow model in actuator disk model
  - ✓ Impingement model : Eulerian approach
  - ✓ Thermodynamic model : water film model

FENSPA-ICE

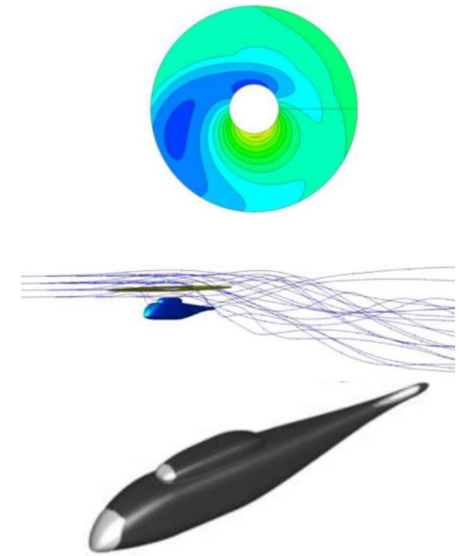

▲ Ice accretion shape with FENSAP-ICE**

- Limitations of previous study
  - ✓ Low fidelity aerodynamic solver, impingement model, and thermodynamic model
  - ✓ Systematic approach is required in various forward speed

*Szilder, K., "Numerical Simulation of Ice Formation on a Helicopter Fuselage," SAE Technical Paper 2007-01-3308, 2007, doi:10.4271/2007-01-3308.
2013, Fouladi, H., Habashi, W. G., and Ozcer, I. A. Quasi-Steady Modeling of Ice Accretion on a Helicopter Fuselage in Forward Flight, Journal of Aircraft, Vol.50, No.4, pp.1169-1178.**

Development of 3D Ice Accretion Code

Numerical approaches to predict ice accretion shapes and its performance

- Expensive to operating and maintain costs of experiment

	1st generation codes	**Limitation of 1st Gen. codes**	**2nd generation codes**
Period	1980~1990s	-	1990s~
Aerodynamic solver	Panel method, Euler equation	(1) Separation flow of high angle of attack, ice horn, cylinder (2) Prediction of aerodynamic force, especially lack of drag prediction	Navier-Stokes equation
Impingement model	Lagrangian approach	No droplet particles in shadow region(flow separation, after ice horn)	Eulerian approach
Thermodynamic mode	2D Messinger model	Sectional approach, axial symmetry problems only	Extended 2D Messinger or 3D water film mode
Representative codes	NASA(LEWICE), ONERA, DRA, CIRA	-	McGill Univ.(FENSAP-ICE), CIRA(ICECREMO)

Goal of this study

- Validation and application of the developed code to 2D and generic 3D icing problems
- Comparison of helicopter fuselage icing with various forward flight speed

Numerical Approach

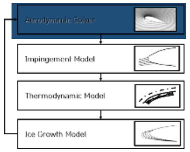

- 4 Models in the platform of open source code(OpenFOAM)
  - Aerodynamic solver, Impingement model, Thermodynamic model, Ice growth model
  - Quasi-steady assumption
    - ✓ One or more iterative calculation of each model
    - ✓ Each model assumed to steady state, and field parts(aerodynamic solver, impingement model) are used local time stepping
    - ✓ Fully converged solution conveyed to next model

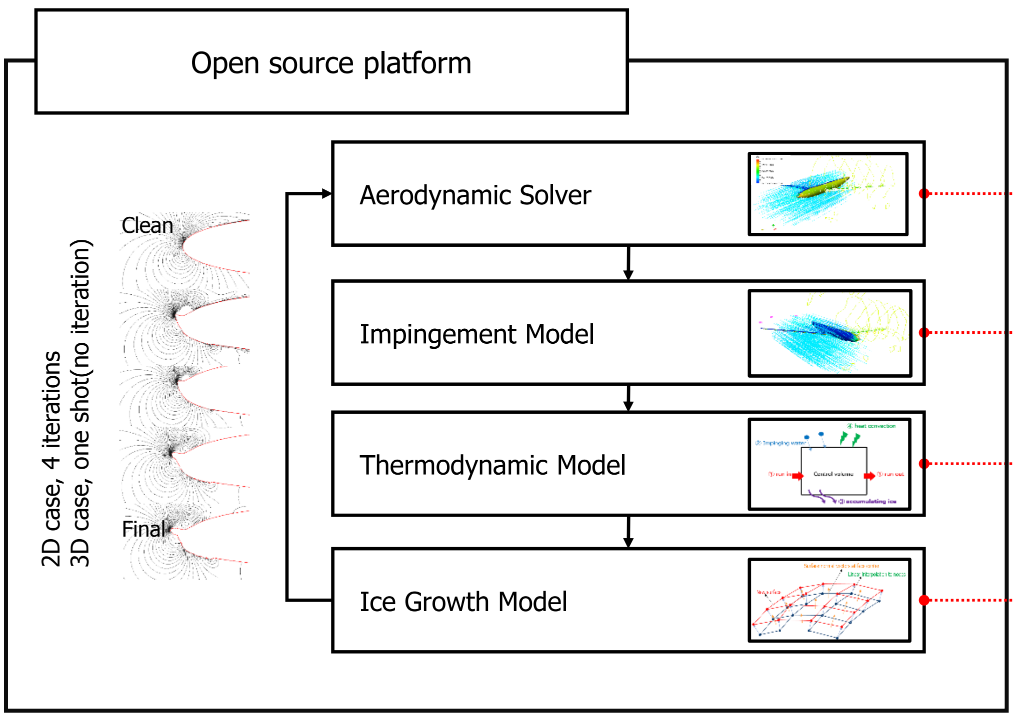

- rhoPimpleFOAM
  - ✓ Navier-Stokes based solver
  - ✓ Unsteady, compressible and turbulent flow
  - ✓ Roughness based S-A model
- 3D Eulerian approach
  - ✓ drag, gravity, and buoyancy forces
- 3D water film approach
  - ✓ FVM method on the surface water film
- 3D surface re-meshing

*Ruff, G. A., and Berkowitz, B. M., *"Users Manual for the NASA Lewis Ice Accretion Prediction Code(LEWICE)," NASA CR-185129, May 1990,* DIANE Publishing, 1990.

Numerical Approach

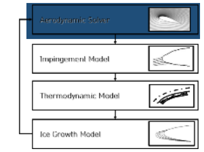

Validation results of aerodynamic solver

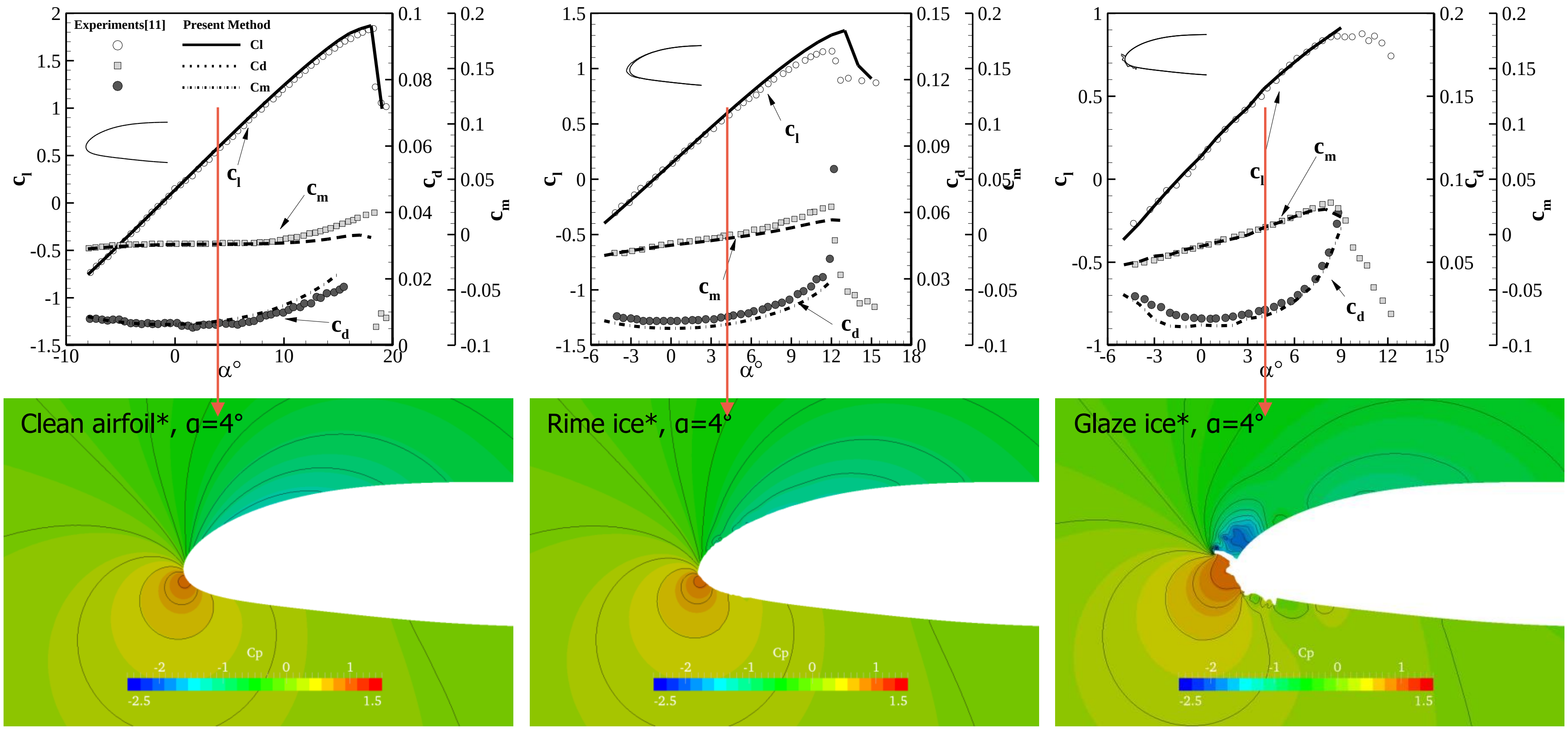

- Flow condition : M_∞=2.0, $Re = 15.9 \times 10^6$, α=4°

- Icing Condition : α=2°, V_∞=77.2m/s, T_∞=-22.2°C, LWC=0.55g/m³, MVD=30μm, time=10min
- Flow condition : M_∞=0.2, $Re = 15.9 \times 10^6$, α=4°

- Icing Condition : α=5°, V_∞=90m/s, T_∞=-2.2°C, LWC=0.85g/m³, MVD=20μm, time=11.3min.
- Flow condition : M_∞=0.2, $Re = 15.9 \times 10^6$, α=4°

*Broeren, P. A., Bragg, M. B., Addy, H. E. Jr., Lee, S., Moens, F., and Guffond, D., "Effect of High Fidelity Ice- Accretion Simulations on Full-Scale Airfoil Performance", Journal of Aircraft, 47(1): 240-254, 2010, doi: 10.2514 / 1.45203.

Numerical Approach

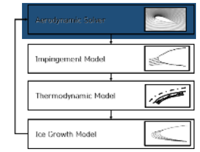

Ice changes surface roughness(k_s)

- Accelerates flow transition, skin friction and heat convection characteristics
- NASA empirical correlation*, k_s=f(T,V,LWC,MVD)

Modified Spalart-Allmars(SA) for surface roughness

- Original SA model(Present method)
  - ✓ $\frac{\partial \tilde{\nu}}{\partial t} + u_j \frac{\partial \tilde{\nu}}{\partial x_j} = c_{b1}(1 - f_{t2})\tilde{S}\tilde{\nu} - \left[c_{w1} f_w - \frac{c_{b1}}{\kappa^2}\right]\left(\frac{\tilde{\nu}}{d}\right)^2 + \frac{1}{\sigma}\left[\frac{\partial}{\partial x_j}\left((\nu + \tilde{\nu})\frac{\partial \tilde{\nu}}{\partial x_j}\right) + c_{b2}\frac{\partial \tilde{\nu}}{\partial x_i}\frac{\partial \tilde{\nu}}{\partial x_i}\right]$
- Current Model : Surface roughness
  - ✓ $d = d_{wall} + 0.03k_s$
- Wall boundary
  - ✓ $\frac{\partial \tilde{\nu}}{\partial n} = \frac{\tilde{\nu}}{d_{new}}$
- Heat convection
  - ✓ $h_c = \frac{-(k_l + k_t)\partial T/\partial n}{T_s - T_\infty}$
  - ✓ $k_t = \frac{\mu_t c_p}{Pr_t}$

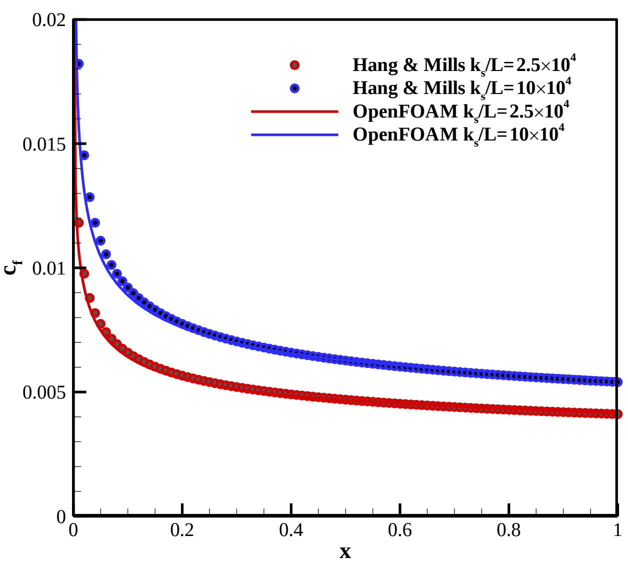

▲ Skin friction coefficient of roughened flat plate

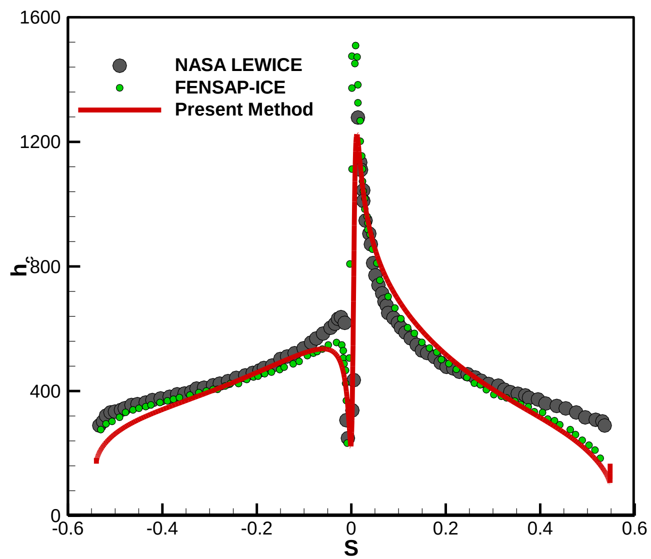

▲ Heat convection coefficient(right) at roughened airfoil

*Ruff, G. A., and Berkowitz, B. M., *"Users Manual for the NASA Lewis Ice Accretion Prediction Code(LEWICE)," NASA CR-185129, May 1990,* DIANE Publishing, 1990.

Numerical Approach

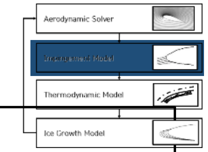

Eulerian Method

- Droplet field is governed by mass and momentum conservation
- Eulerian approach is suitable for FVM, FEM method
  - ✓ Shadow region is automatically calculated

- Mass Conservation
  - ✓ $\frac{\partial \bar{\rho}_d}{\partial t} + \nabla \cdot (\dot{\rho}_d \vec{u}_d) = 0$
    - $\bar{\rho}_d = \alpha \rho_w$
    - $\bar{\rho}_d$: bulk density, α : volume fraction

- Momentum conservation
  - ✓ $\frac{\partial \bar{\rho}_d \vec{u}_d}{\partial t} + \nabla \cdot (\dot{\rho}_d \vec{u}_d \vec{u}_d) = \underbrace{\frac{3}{4}\frac{\bar{\rho}_d \mu_a C_D Re_d}{\rho_w MVD^2}(\vec{u}_a - \vec{u}_d)}_{\text{drag}} + \underbrace{\dot{\rho}_d \vec{g}\left(1 - \frac{\rho_a}{\rho_w}\right)}_{\text{gravity, and buoyancy}}$
    - $C_D = 24/Re_d\left(1 + 0.197 Re_d{}^{0.63} + 2.6 \times 10^{-4} Re_d{}^{1.38}\right)$

- Collection efficiency
  - ✓ $\beta = \frac{\bar{\rho}_d \vec{u}_d \cdot \vec{n}}{LWC \cdot U}$

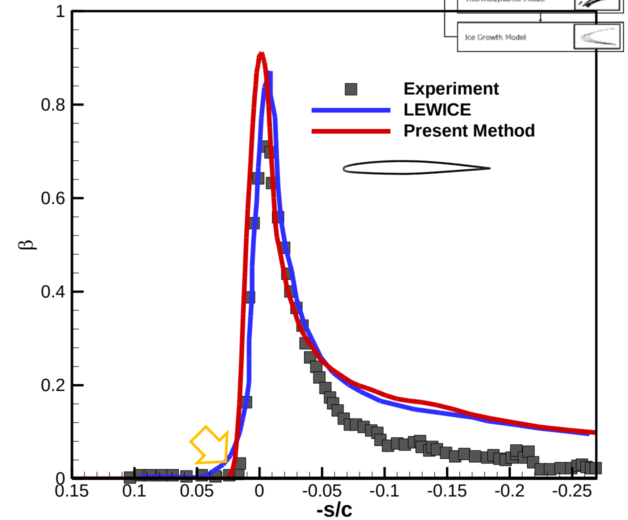

▲ Collection efficiency of GLC305*

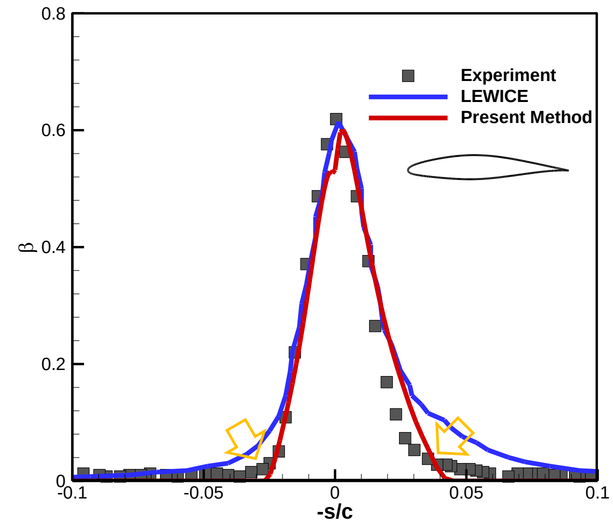

▲ Collection efficiency of NACA64$_A$014*

*Papadakis, M., Hung, K. E., Vu, G. T., Yeong, H. W., Bidwell, C. S., Breer, M. D., and Bencic, T. J., *Experimental Investigation of Water Droplet Impingement on Airfoils, Finite Wings, and an S-Duct Engine Inlet*, NASA Technical Memorandum, 2002.

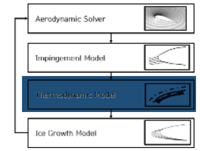

Governing equations

- Mass conservation — 2 Unknowns : $h_f, \dot{m}_{ice}$
  - ✓ ① run in and out(runback water), ② Impinging water, ③ accumulating ice
  - ✓ $\rho_w \left[\int \frac{\partial h_f}{\partial t} dV + \underbrace{\int \nabla \cdot (h_f \bar{U}_f) dV}_{①} \right] = \underbrace{\dot{m}_{com}}_{②} - \underbrace{\dot{m}_{ice}}_{③}$
- Energy conservation — 3 Unknowns : $h_f, \dot{m}_{ice}, \tilde{T}_{eq}$
  - ✓ ① run in and out(runback water), ② impinging water(kinetic energy), ③ accumulating ice(latent heat), ④ heat convection
  - ✓ $\rho_w \left[\int \frac{\partial h_f c_{p,w} \tilde{T}_{eq}}{\partial t} dV + \underbrace{\int \nabla \cdot (h_f c_{p,w} \tilde{T}_{eq} \bar{U}_f) dV}_{①} \right] = \underbrace{\dot{m}_{com} \left[c_{p,w} \tilde{T}_{d,\infty} + \frac{1}{2} U_d^2 \right]}_{②} + \underbrace{\dot{m}_{ice} \left[L_{fus} - c_{p,i} \tilde{T}_{eq} \right]}_{③} + \underbrace{h_c (T_{eq} - T_\infty)}_{④}$

→ Momentum conservation — $\bar{U}_f = f(h_f)$

- ✓ $\bar{U}_f = f(h_f) = \frac{1}{h_f} \int_0^{h_f} u_f dh = \frac{h_f}{2\mu_w} \vec{\tau}_{wall}$
  - $\rho_w A h_f = \rho_h V$, $h_f = \rho_h V / \rho_w A$

Compatibility relations

- Unknowns : h_f, $\tilde{T}_{eq}$, $\dot{m}_{ice}$
- 2 Equations : Mass and energy conservation
  - ✓ Not enough to determine the unknowns
  - ✓ **Additional compatibility relations** are required

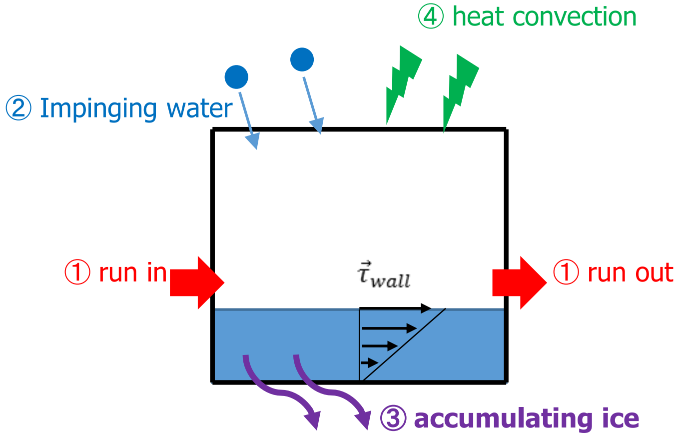

NUMERICAL APPROACH

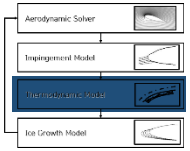

3 compatibility relations

- Compatibility relations are based on physical observations
- From the surface condition, 1 unknown determined → the other 2 unknows explicitly calculated
- Apply each surface condition at each surface cell and check the compatibility relations

> ✓ Water only : $\tilde{T}_{eq} \geq 0°\mathrm{C}, \dot{m}_{ice}, = 0, h_f \geq 0$
> ✓ Water & Ice : $\tilde{T}_{eq} = 0°\mathrm{C}, \dot{m}_{ice} \geq 0, \mathrm{h}_f \geq 0$
> ✓ Ice only : $\tilde{T}_{eq} \leq 0°\mathrm{C}, \dot{m}_{ice}, \geq 0, \mathrm{h}_f = 0$
>
> Time step : n+1

- From the surface temperature of previous time step($\tilde{T}_{eq}{}^{n}$), application order is determined
  - ✓ If $\tilde{T}_{eq}{}^{n} < 0°\mathrm{C}$
    - (3) Ice only → (2) Water & Ice → (1) Water only
  - ✓ Else if $\tilde{T}_{eq}{}^{n} \geq 0°\mathrm{C}$
    - (1) Water only → (2) Water & Ice → (3) Ice only

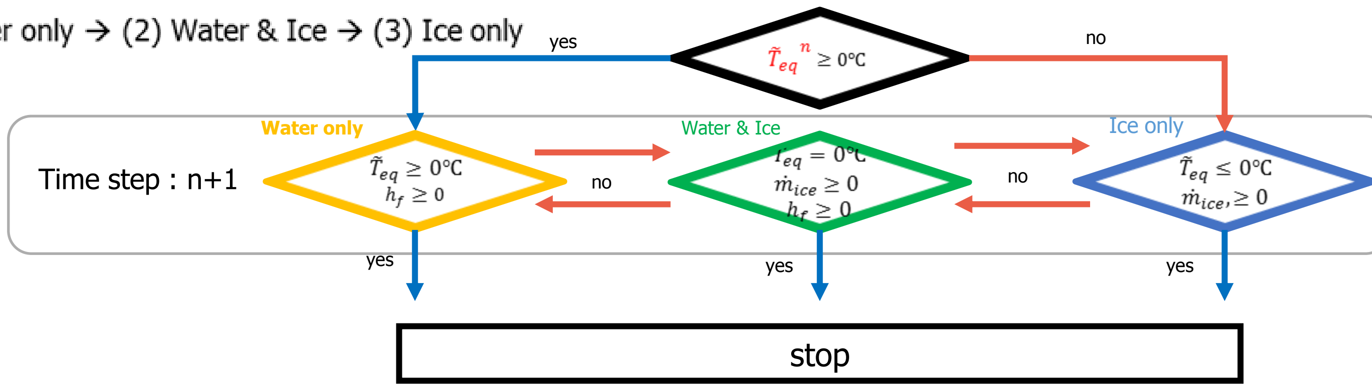

Numerical Approach

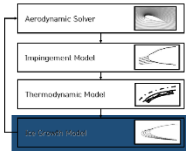

3D Grid generation

- Linear interpolation from face to point
  - ✓ Face values : ice thickness, surface normal vector
- Update surface geometry and re-meshing

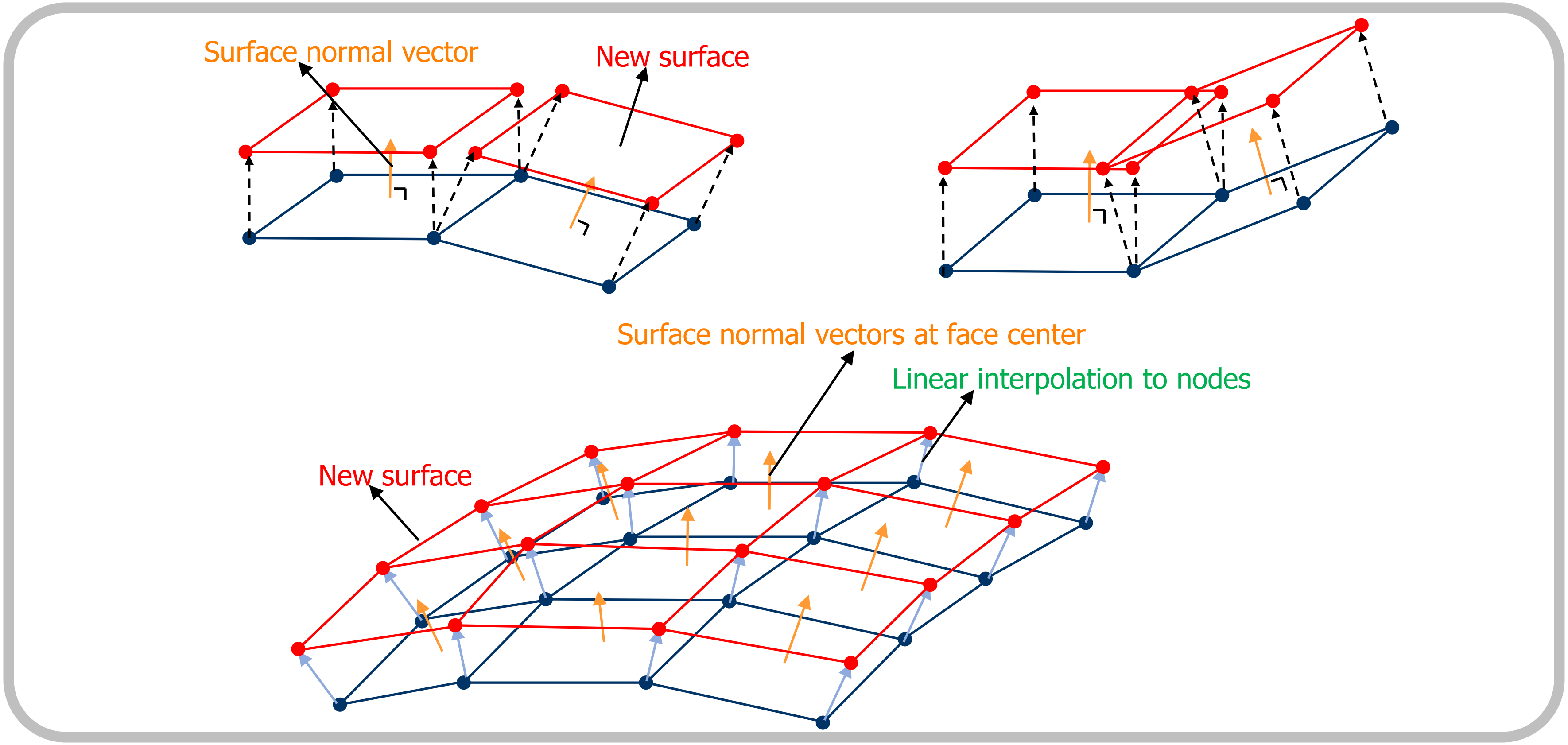

DLRF4 Wing + Fuselage

- Aerodynamic solver
  - Surface pressure and pressure contour

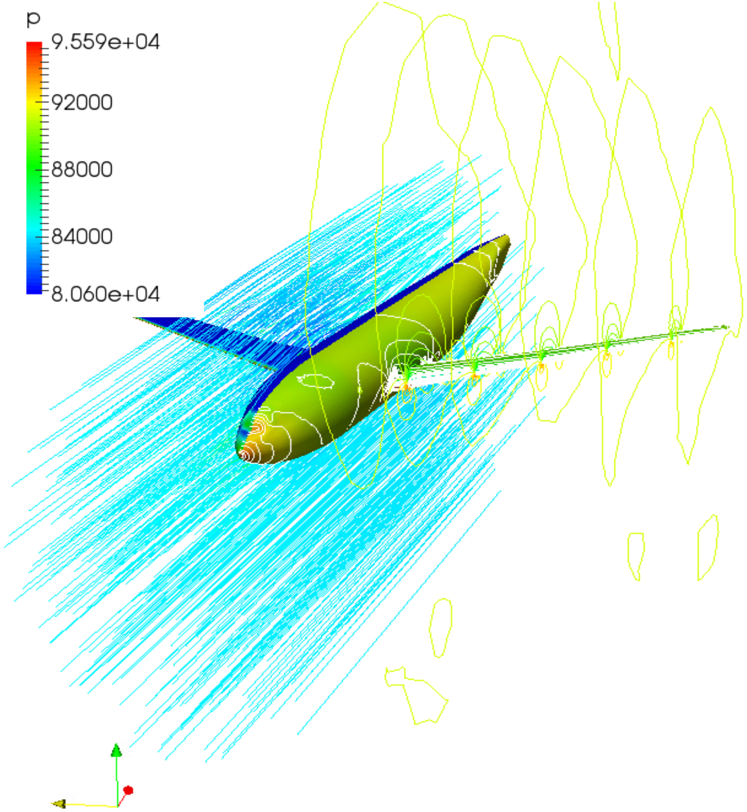

- Impingement model
  - Collection efficiency and droplet trajectory

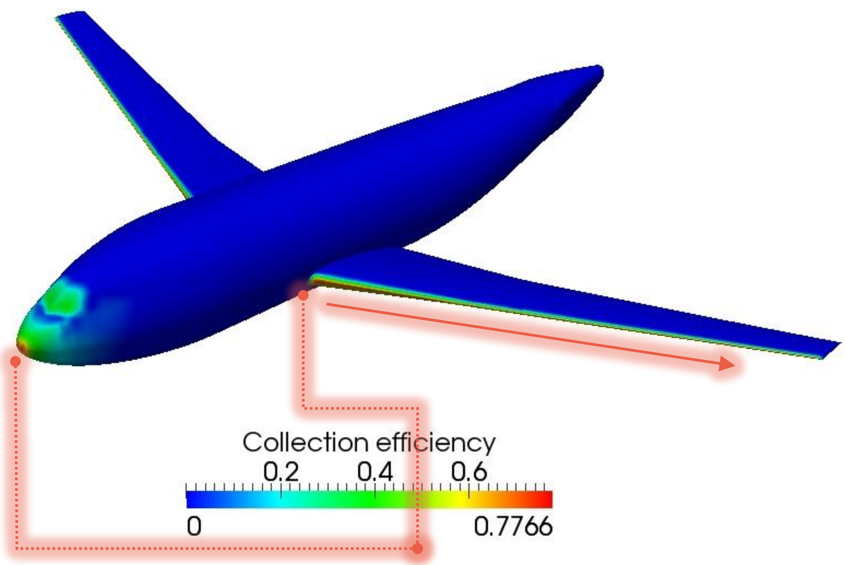

- Maximum location of collection efficiency
  - ✓ Nose of fuselage and leading edge of wing root
- $0 < \beta < 0.78$
  - ✓ The rage of collection efficiency in general airfoils
- Along the leading edge, high value of collection efficiency

Results and Discussion

Ice accumulated aircraft

Fuselage : 1.1902m
Span : 1.171m
Icing Time : 180s
Total ice mass : 87.2g

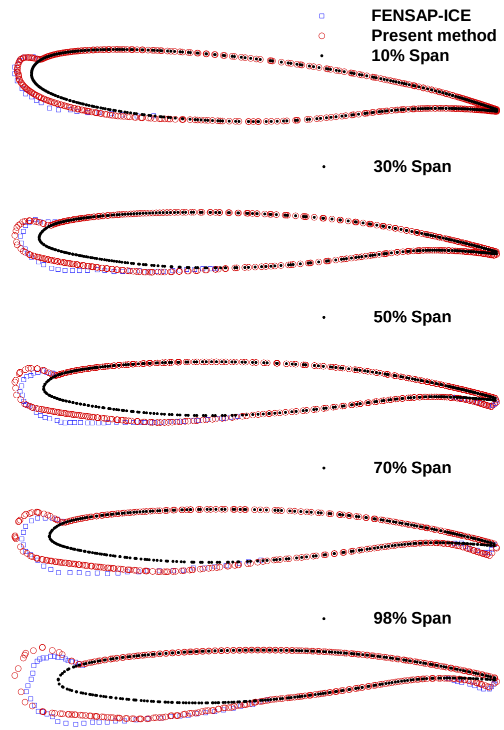

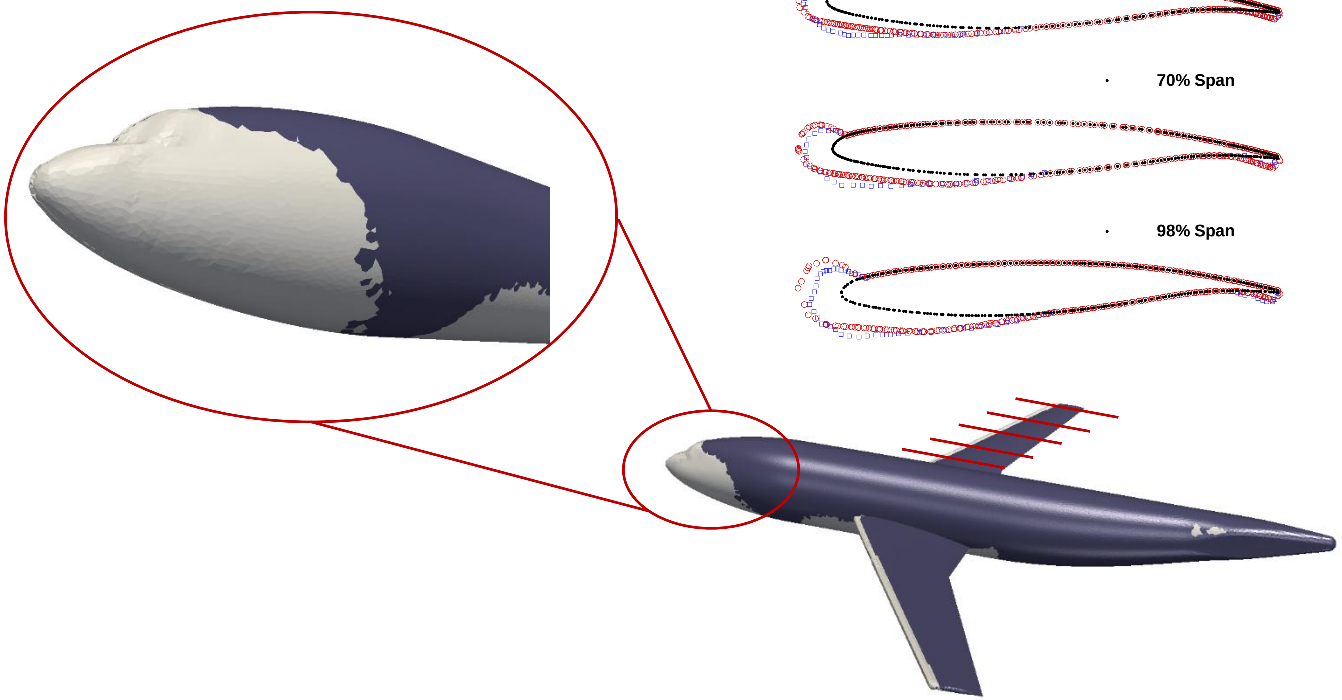

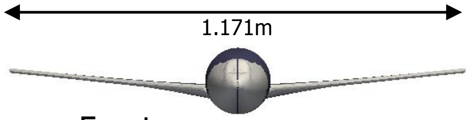

▲ Front

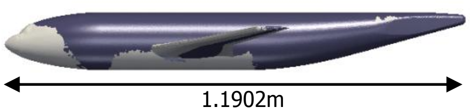

▲ Side

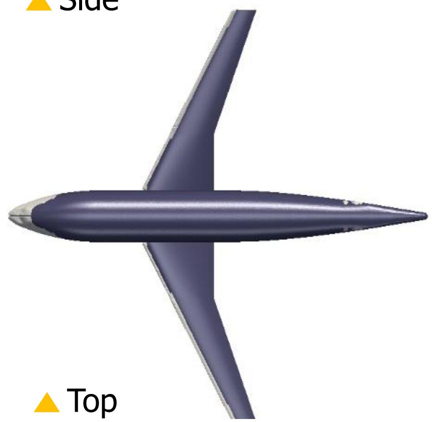

▲ Top

▲ bottom

ROBIN Fuselage Icing

Helicopter fuselage icing*

- Aerodynamic solver
  - ✓ The most time consumption step
  - ✓ Helicopter calculation requires calculation costs
    - Fixed(Fuselage) and rotating(rotor) parts
  - ✓ Icing code needs many iterations
- Actuator disk and actuator surface method
  - ✓ Calculation time efficiency and reliability

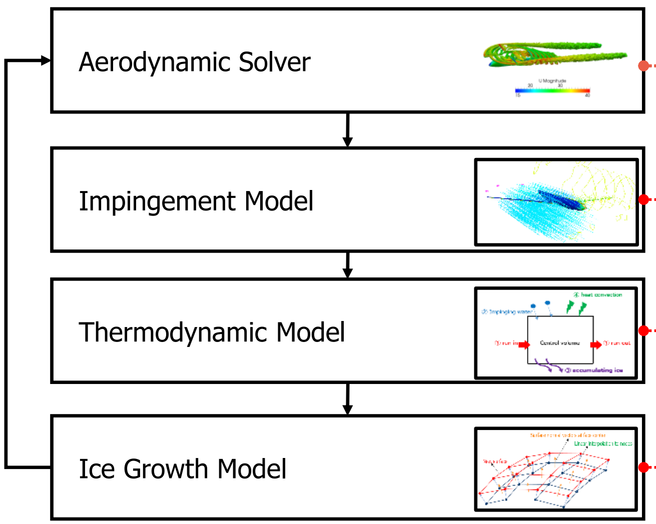

▼ Elliot $\mu = 0.15, U_\infty = 27.035\frac{m}{s}, LWC = 0.7\frac{g}{m^3}, T_\infty = -5°C$

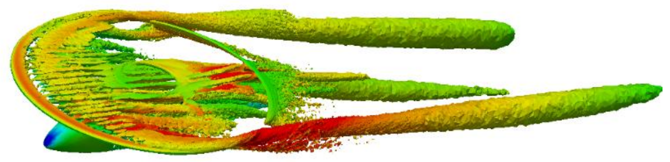

▲ Actuator disk model(ADM)

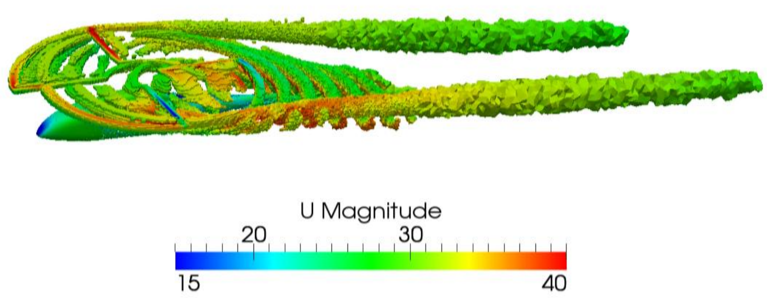

▲ Actuator surface model(ASM)

- Same procedures with fixed wing aircraft

Elliot, J., Althoff, S. L., Sailey, R., "Inflow Measurement Made with a Laser Velocimeter on a Helicopter Model in Forward Flight, Vol. 1. Rectangular Planform Blades at an Advance Ratio of 0.15," NASA TM 100541, 1987

ROBIN Fuselage Icing

ADM vs ASM

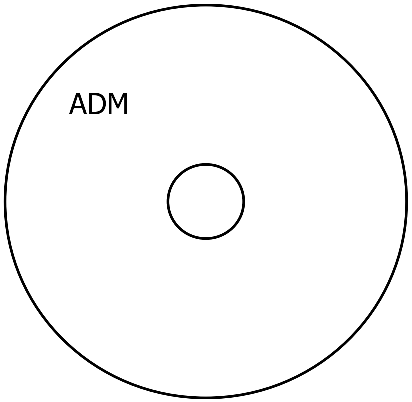

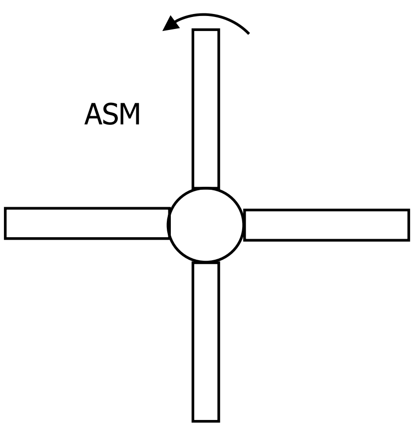

Properties on the surface

Property in the field

Elliot case $\mu = 0.15$

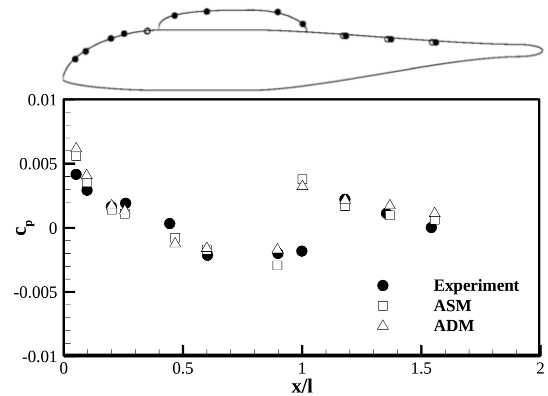

Surface pressure distribution

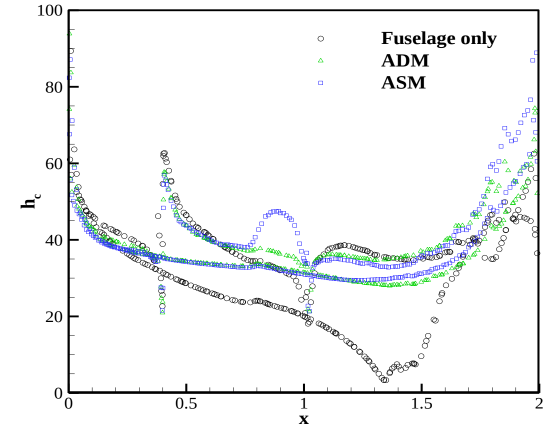

Heat convection coefficient

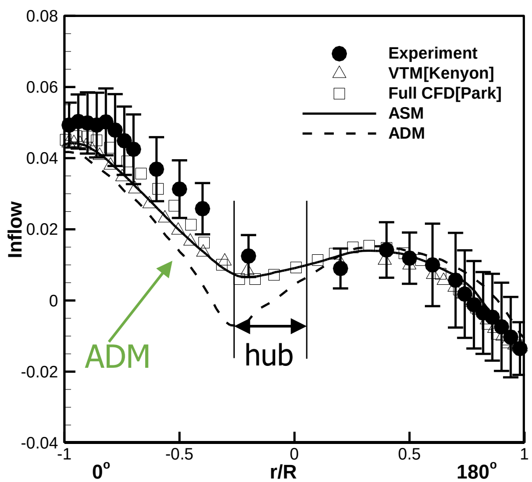

longitudinal inflow distribution

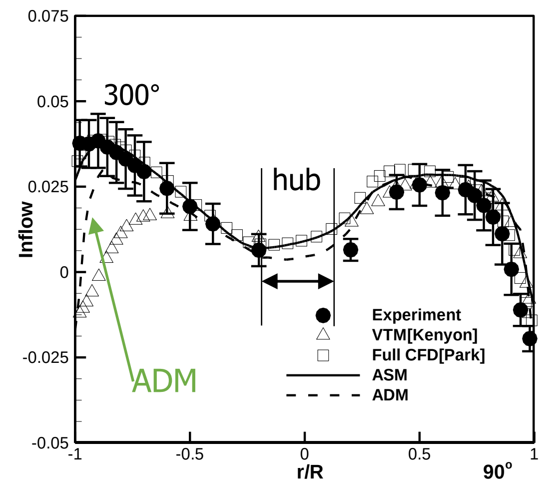

Lateral inflow distribution

Elliot, J., Althoff, S. L., Sailey, R., "Inflow Measurement Made with a Laser Velocimeter on a Helicopter Model in Forward Flight, Vol. 1. Rectangular Planform Blades at an Advance Ratio of 0.15," NASA TM 100541, 1987

ROBIN Fuselage Icing

Collection efficiency and ice accretion shapes

- $\mu = 0.0, 0.075, 0.15$
- $LWC = 0.7\frac{g}{m^3}, T_\infty = -5°\mathrm{C}$

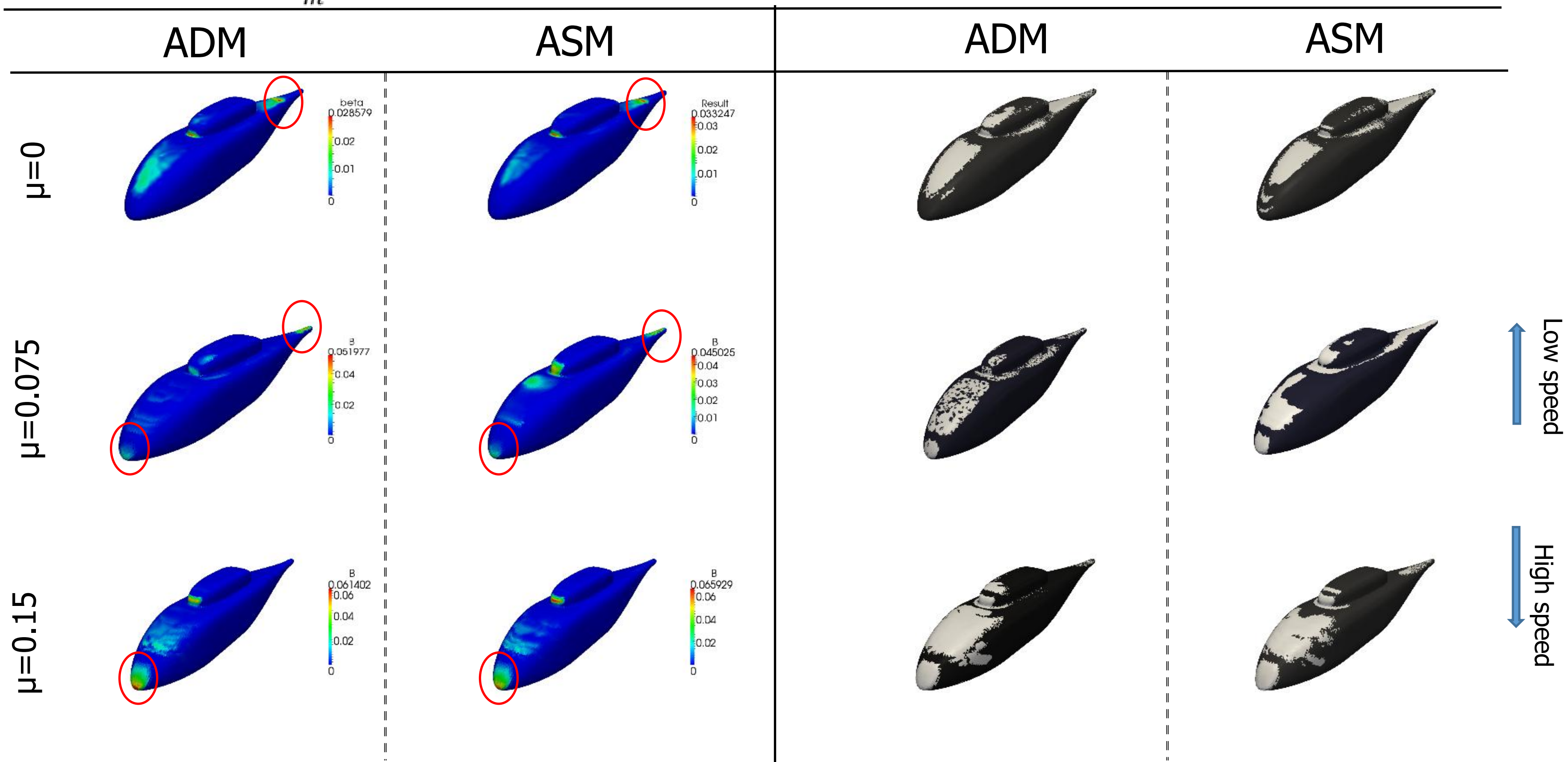

Collection efficiency, $\beta = \frac{\overline{\rho}_d \vec{u}_d \cdot \vec{n}}{LWC \cdot U}$

Ice accretion shapes

ROBIN Fuselage Icing

- Hovering

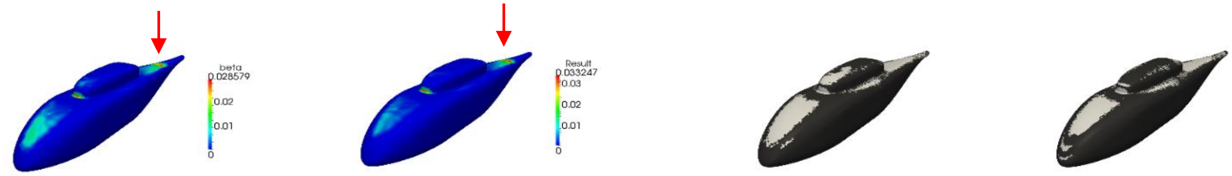

ADM	ASM $\beta_{max(ASM)} > \beta_{max(ADM)}$, 16%

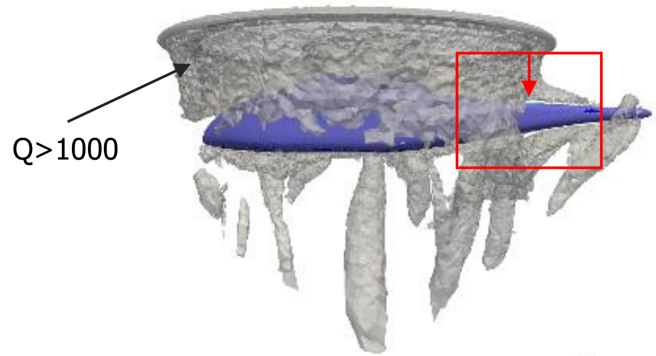

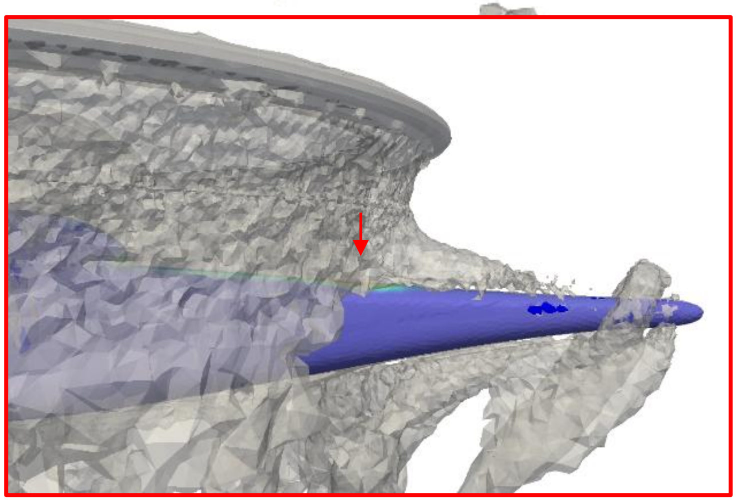

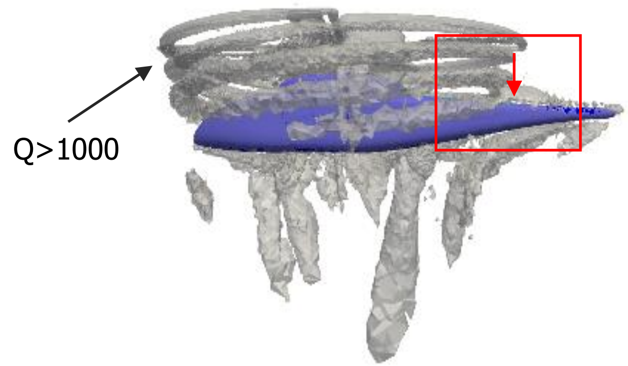

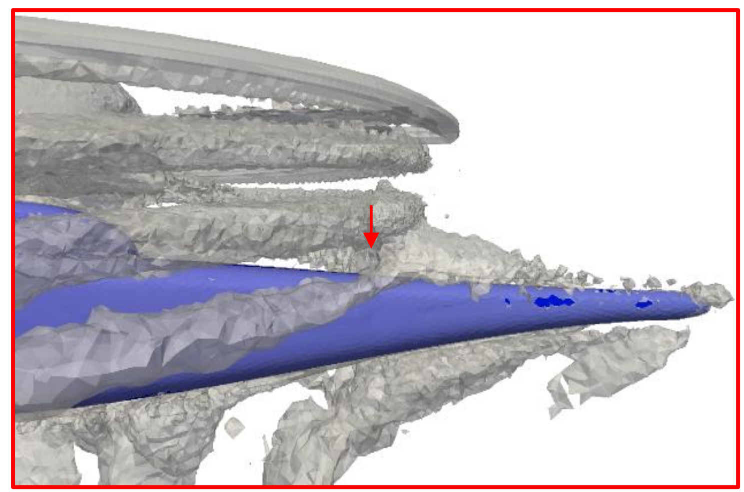

ROBIN Fuselage Icing

- $\mu = 0.075$

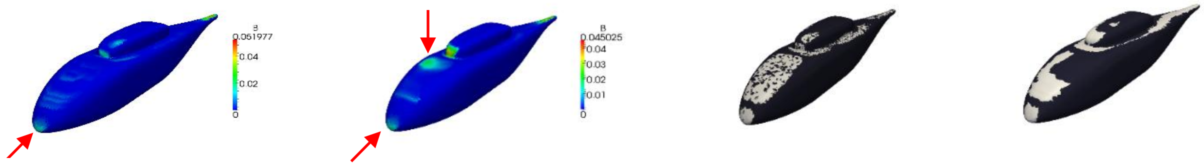

ADM	ASM $\beta_{max(ASM)} < \beta_{max(ADM)}$, 2%

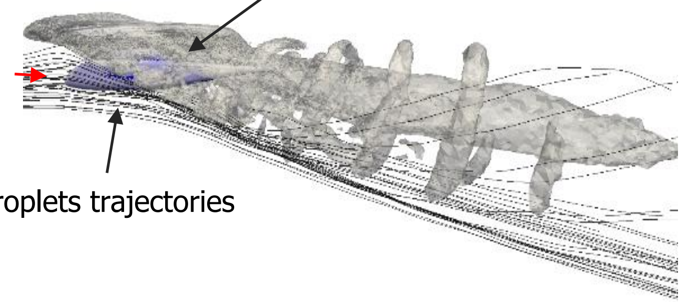

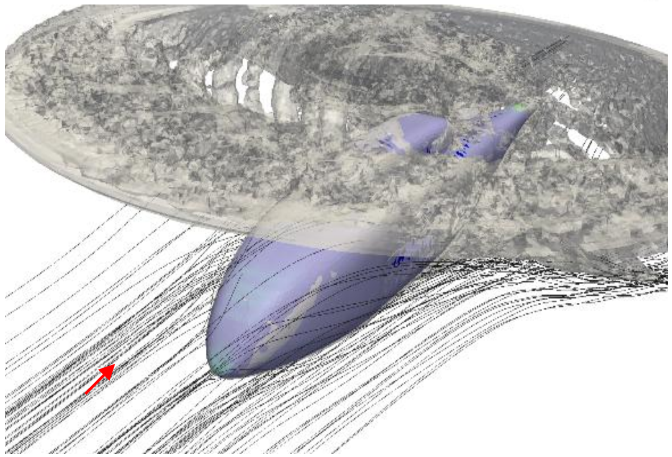

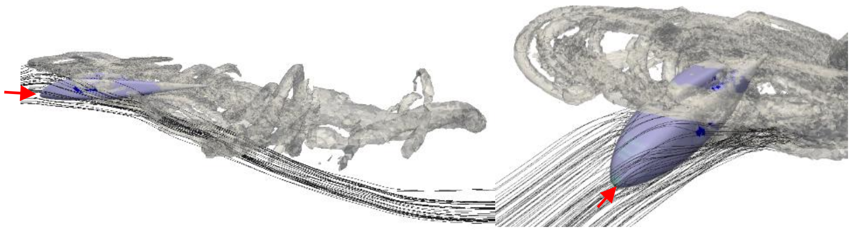

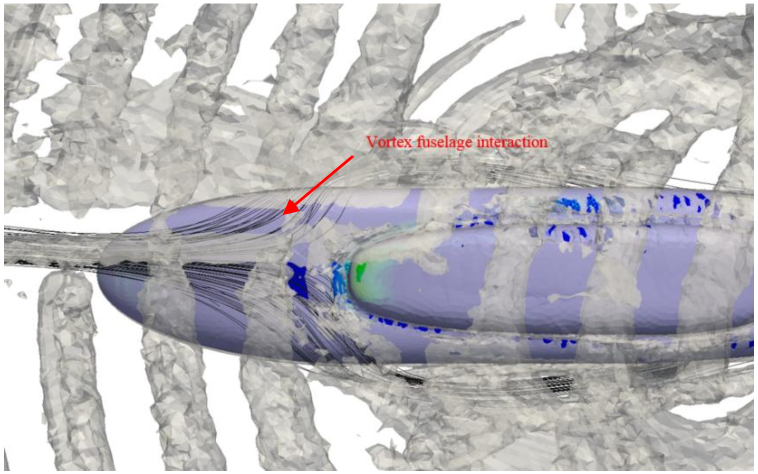

ROBIN Fuselage Icing

- $\mu = 0.075$

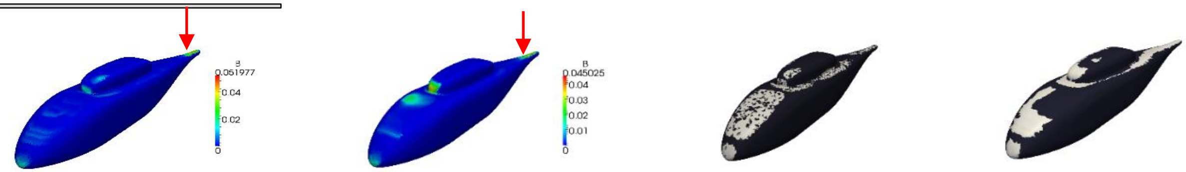

ADM	ASM

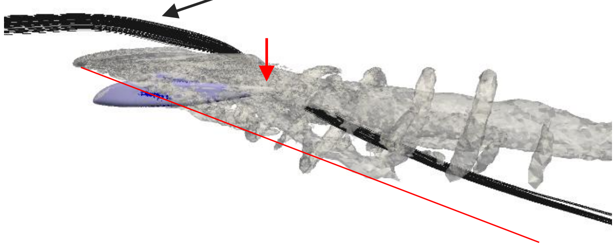

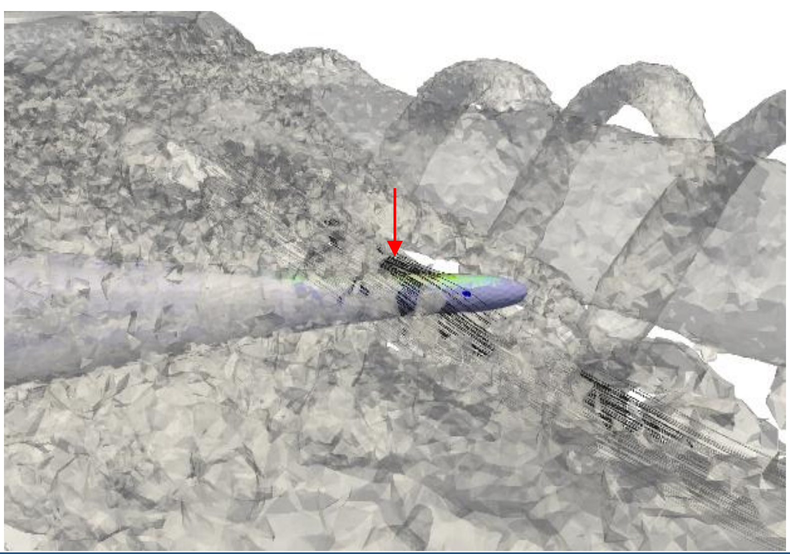

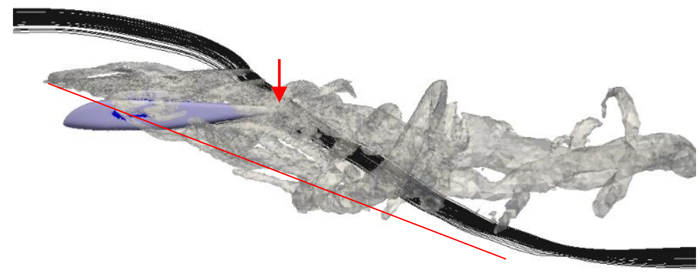

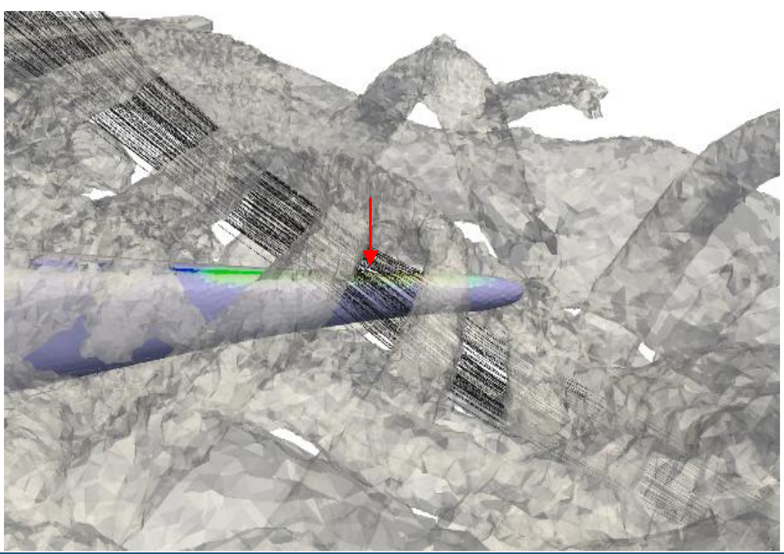

ROBIN Fuselage Icing

- $\mu = 0.15$

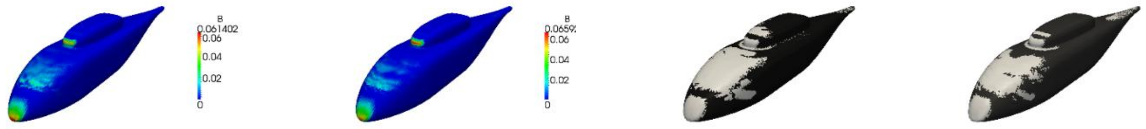

ADM	ASM $\beta_{max(ASM)} > \beta_{max(ADM)}$, 7.3%

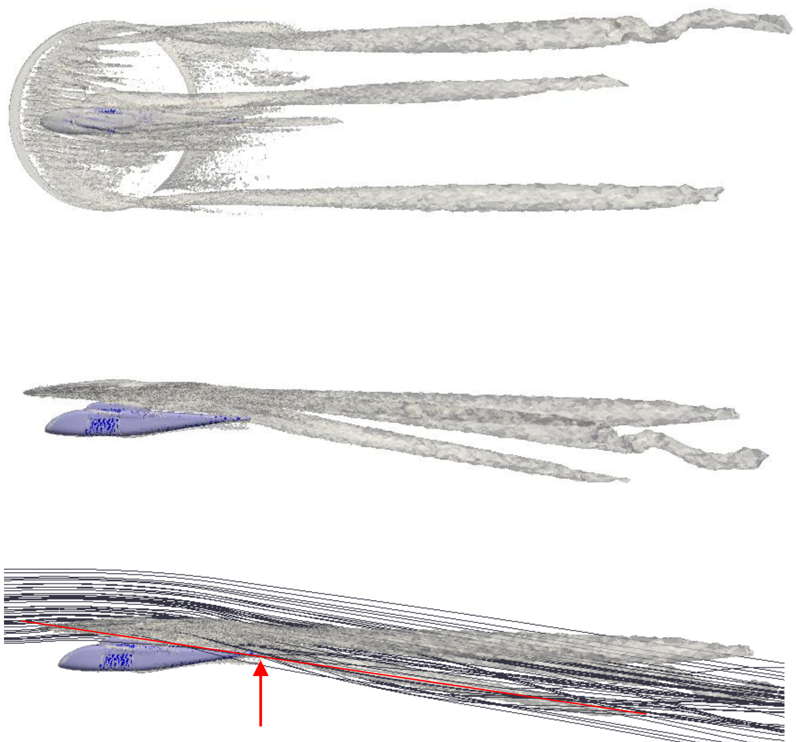

Tip of fuselage

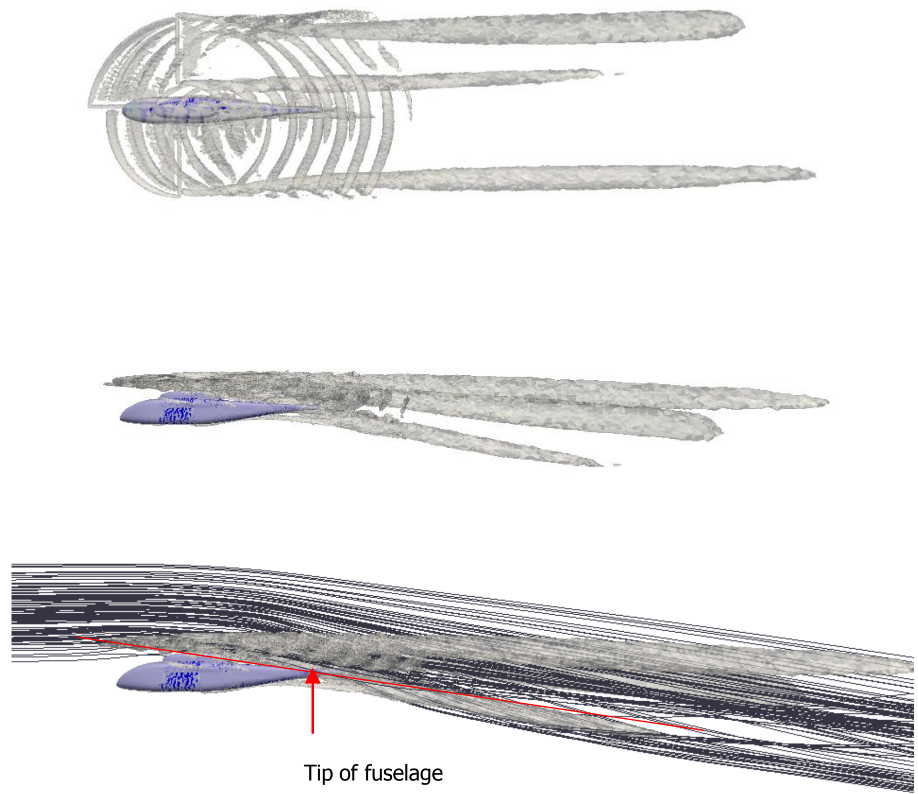

Tip of fuselage

ROBIN Fuselage Icing

- $\mu = 0.15$

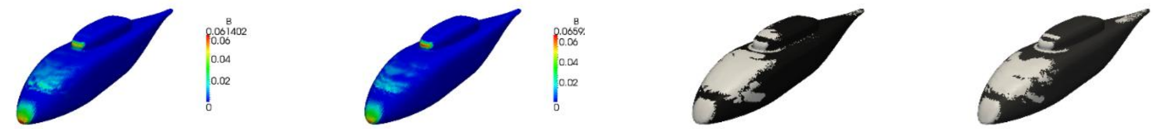

ADM	ASM
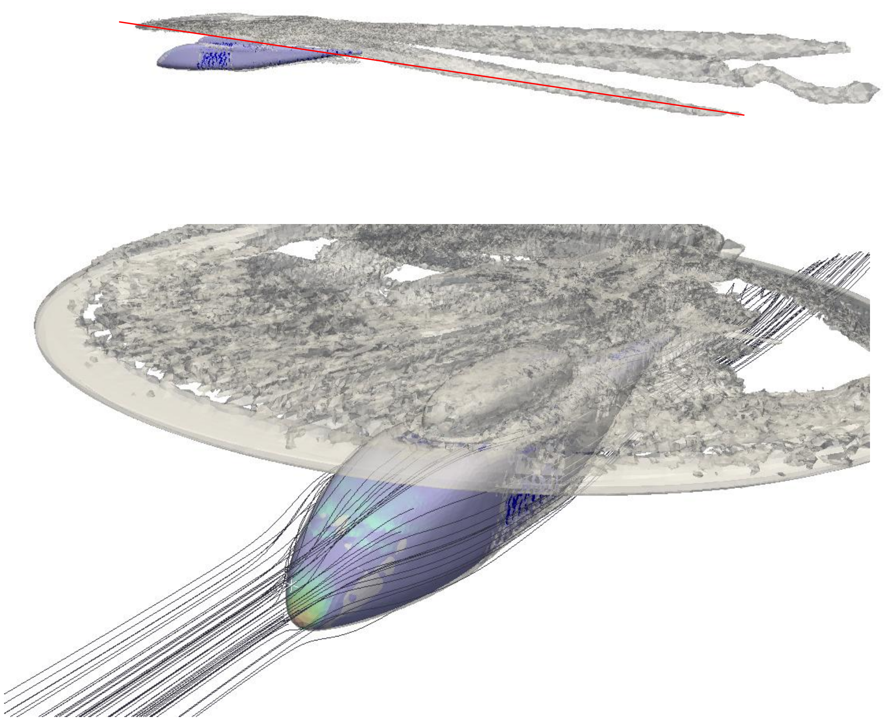	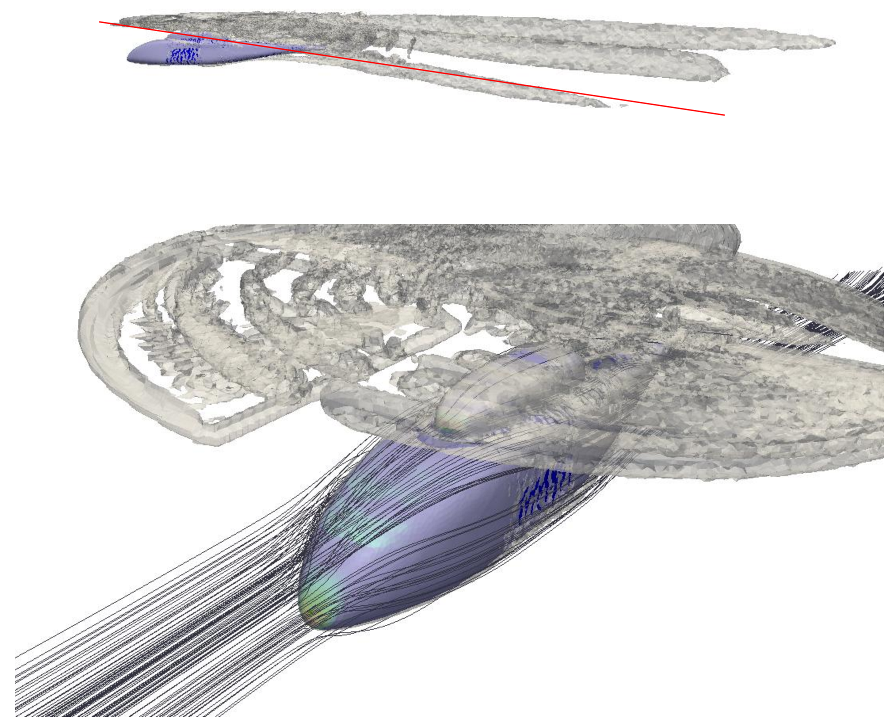

Summary

Forward flight speed

- Hovering, low speed, and high speed forward flight conditions are simulated
- As increasing the forward flight speed, the pattern of ice shapes are different.
  - ✓ Hovering : tail boom and wind shield
  - ✓ Low speed forward flight : fuselage nose and tail boom
  - ✓ High speed forward flight : fuselage nose and wind shield
    - The effect of the forward flight speed is more dominant than that of rotor wake

Rotor modeling

- Actuator disk model(ADM) and actuator surface models(ASM) are compared
  - ✓ Ice shapes and distribution of collection efficiency are not significantly different qualitatively
  - ✓ Wake body interaction make high collection efficiency
    - It is essential to predict the behavior of tip vortex rollup and vortex sheet for accurate wake body interaction
    - We consider that the results of ASM are more accurate than those of ADM
      - ASM is modeling the behavior of tip vortex and vortex sheets

ROBIN Fuselage Icing

- The effect of rotor analysis *
  - $\mu = 0.15, U_\infty = 27.035\frac{m}{s}, LWC = 0.7\frac{g}{m^3}, T_\infty = -5°C$
  - Comparison of collection efficiency and ice accretion shapes with and without rotor

Fuselage only

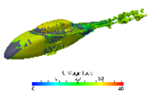

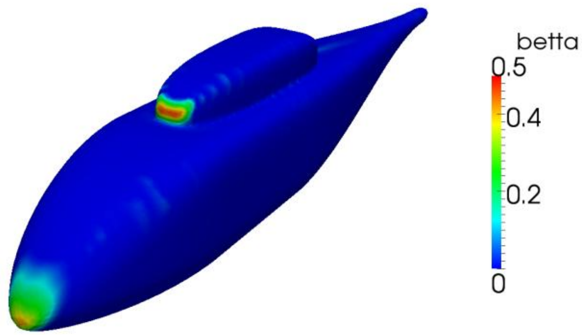

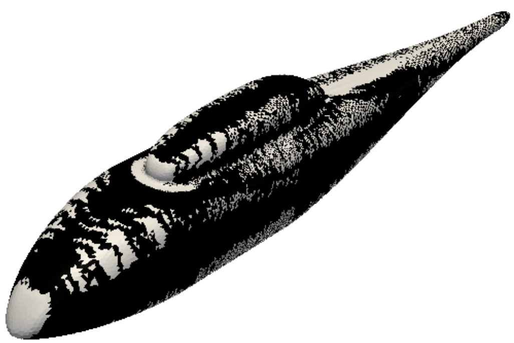

Rotor+fuselage

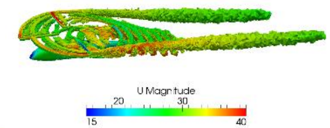

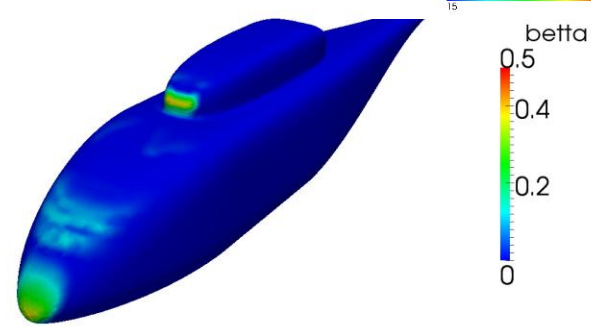

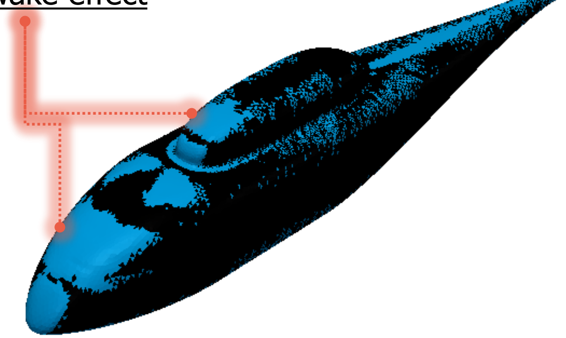

Elliot, J., Althoff, S. L., Sailey, R., "Inflow Measurement Made with a Laser Velocimeter on a Helicopter Model in Forward Flight, Vol. 1. Rectangular Planform Blades at an Advance Ratio of 0.15," NASA TM 100541, 1987

ROBIN Fuselage Icing

- Helicopter fuselage icing
  - Without rotor case is heavier than with rotor case

With rotor : 30.0g, less than 20%

Without rotor : 37.8g

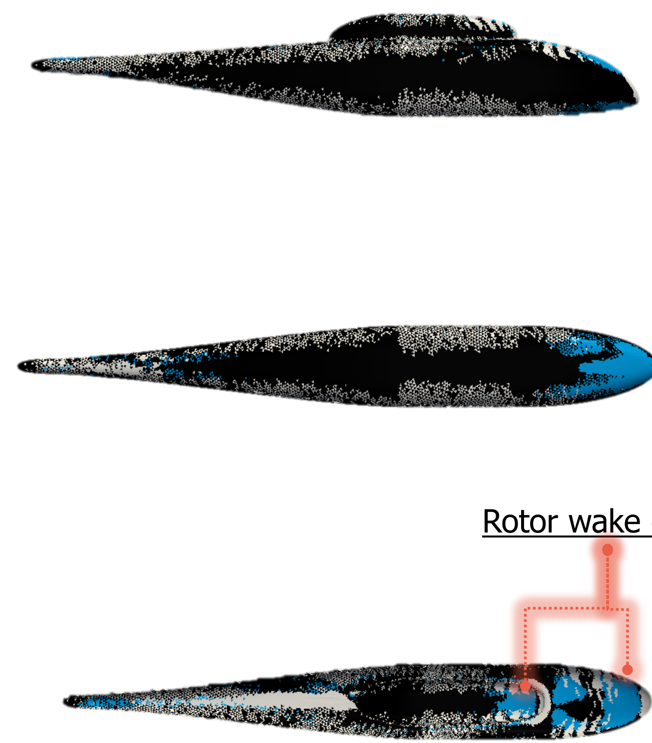

ROBIN Fuselage Icing

Flow field

Fuselage only

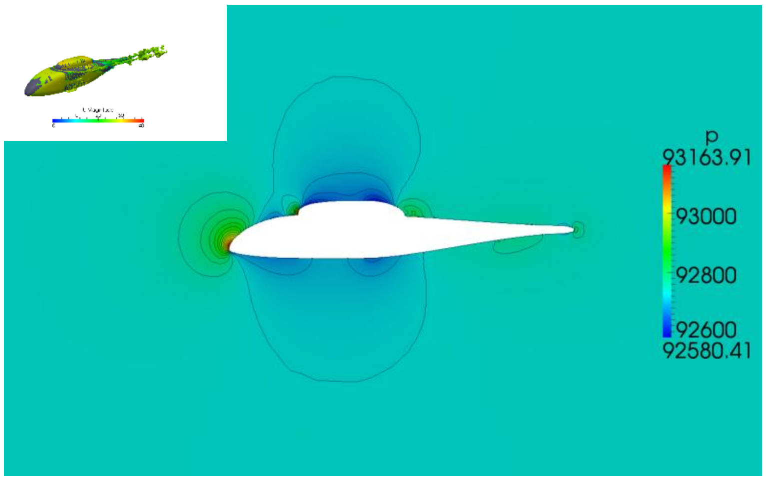

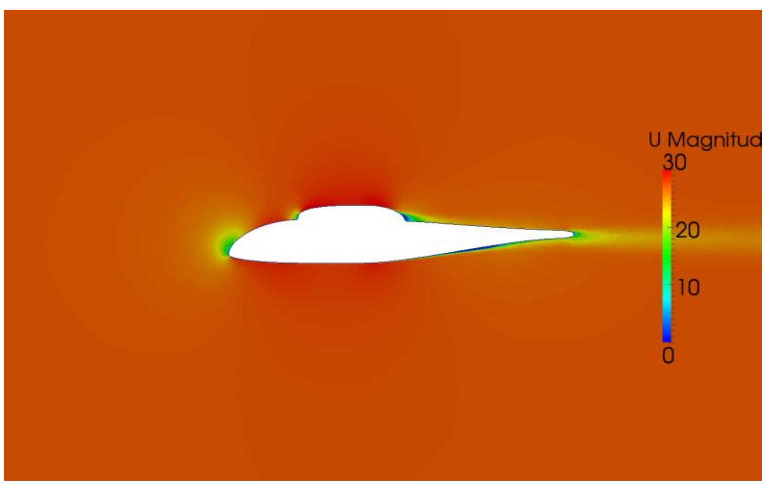

Rotor+fuselage

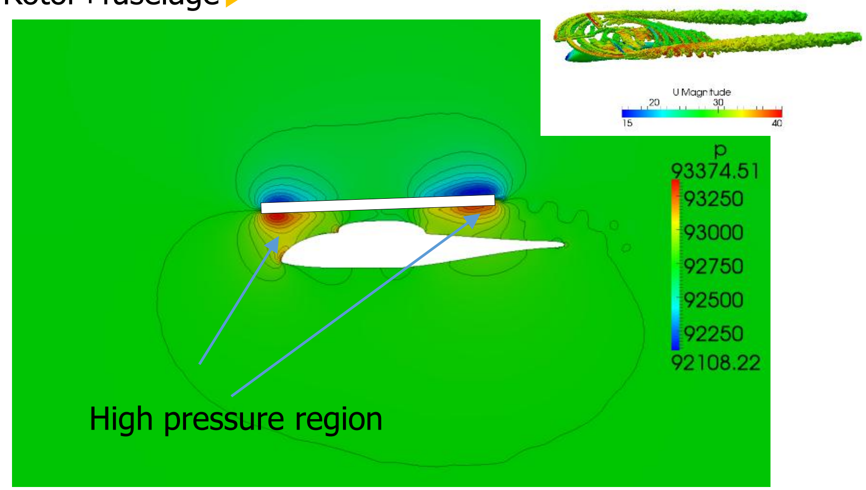

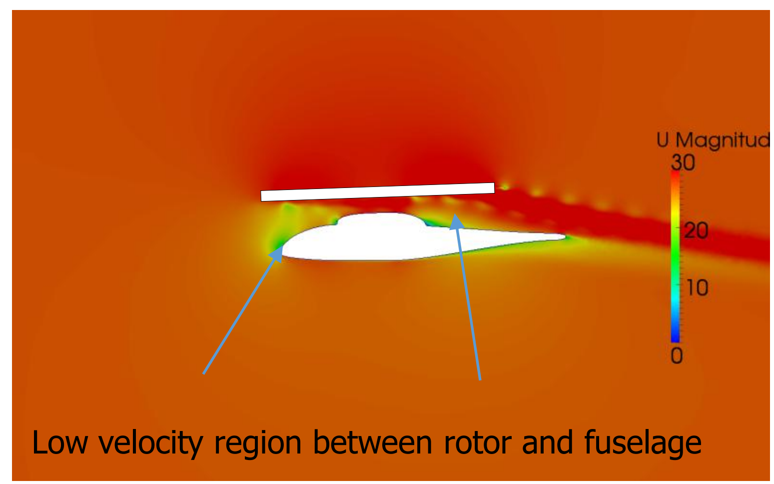

ROBIN Fuselage Icing

Particle trajectory

- Momentum conservation

Low velocity region

✓ $$\frac{\partial \bar{\rho}_d \vec{u}_d}{\partial t} + \nabla \cdot (\bar{\rho}_d \vec{u}_d \vec{u}_d) = \frac{3}{4} \frac{\bar{\rho}_d \mu_a C_D Re_d}{\rho_w MVD^2} \underline{(\vec{u}_a - \vec{u}_d)} + \bar{\rho}_d \vec{g} \left(1 - \frac{\rho_a}{\rho_w}\right)$$

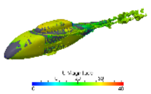

Fuselage only

Rotor+fuselage

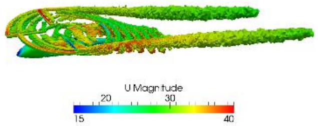

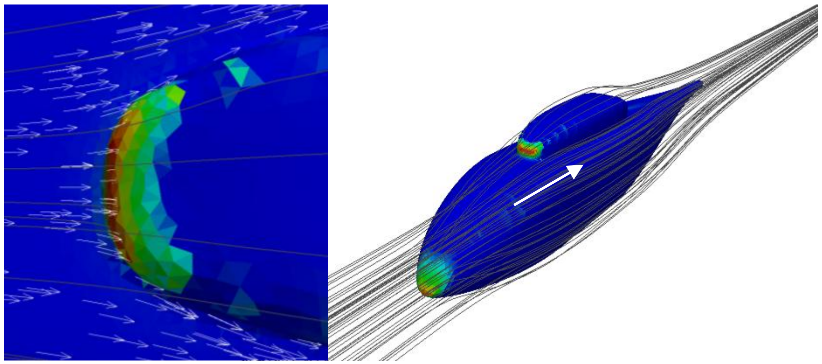

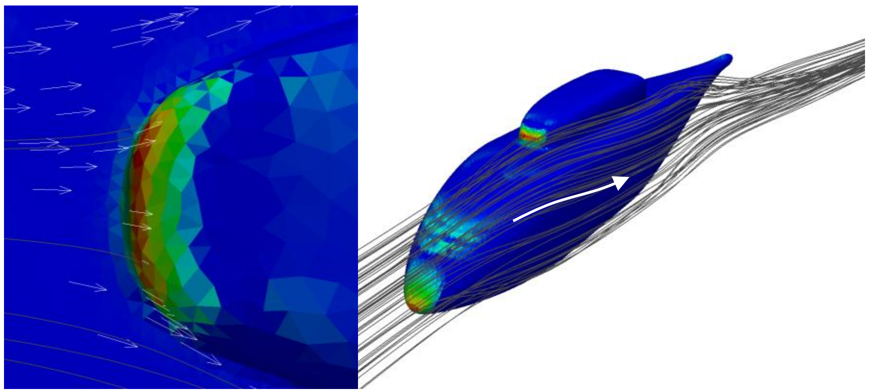

Straight path of particle → impinging

Particle can avoid the fuselage

CONCLUSION

Conclusion

- Development of 3D Ice Accretion Code Based on Eulerian approach
  - 2D problem : Glaze ice(including ice horn), and rime ice condition
    - ✓ Similar accuracy with NASA LEWICE, FENSAP_ICE, and icing wind tunnel tests
  - Generic 3D problems : DLR-F4(wing and fuselage) cases
    - ✓ Ice heading direction, and maximum thickness are well predicted
  - Not enough capability around lower surface
    - ✓ Turbulent effect to the impinging model
    - ✓ Heat convection coefficient of lower surface

- Rotorcraft fuselage icing problem
  - Rotor wake effect should be considered – windshield, engine cowl, tail boom icing
    - ✓ Particle trajectories and mass of accumulated ice on the surface are different
  - As increasing the forward flight speed, the pattern of ice shapes are different.
  - Predicted ice shapes and distribution of collection efficiency by ASM and ADM are not significantly different qualitatively
    - ✓ Additional research is necessary for quantitative analysis

경청해 주셔서 감사합니다.

Conclusion

- View point of an aerodynamicist
  - There are lots of applicable parts to CFD in aviation safety
  - AVDL focused on wake vortex turbulence and aircraft icing
- Topic 1, Wake vortex turbulence
  - (1) Development of novel passive equipment, chipped wing tip shape, to attenuate the vortex intensity
    - ✓ A strong counter-rotating vortex is formed at the edge of the chip, which is eventually merged into a single vortex with substantially less strength.
    - ✓ There is a trade-off relationship between increment of drag and the decrement of vortex intensity
  - (2) Wake vortex warning systems
    - ✓ Research for compatibility of both secure aviation safety and efficient use of airports
    - ✓ Real time visualization of wake vortex from high fidelity NS-LES code and data assimilation method
    - ✓ Proving information of wake hazard area to air traffic controllers
- Topic 2, Aircraft icing
  - (1) Relational Analysis
    - ✓ Lift and drag penalties in glaze ice condition
    - ✓ Moment penalties in rime ice condition
  - (2) Development of 2^{nd} Generation 3D icing code
    - ✓ 2D problem : Glaze ice(including ice horn), and rime ice condition
      - Similar accuracy with NASA LEWICE, FENSAP_ICE, and icing wind tunnel tests
    - ✓ Generic 3D problems : DLR-F4(wing and fuselage) cases
      - Ice heading direction, and maximum thickness are well predicted
    - ✓ Rotorcraft fuselage icing prediction
      - Rotor wake effect should be considered – windshield, engine cowl, tail boom icing

Motivation

- Aircraft icing
  - Super-cooled liquid water droplets impact and freeze on the aircraft surface
  - Aircraft, helicopter, wind turbine blade, ship, and power line
- Accumulated ice changes surface roughness, and deforms the wing shapes
  - Degradation of left, drag and moment performance
  - Negative to control ability, stall margin, and stall speed
- Major cause of aircraft accidents
  - Aircraft Owners and Pilots Association(AOPA) report : 1990～2000, 3230 accidents are concerned with weather conditions
  - 388 accidents(12%) are related to aircraft icing phenomenon
- Numerical approaches to predict ice accretion shapes and its performance
  - Expensive to operating and maintain costs of experiment

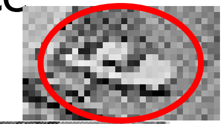

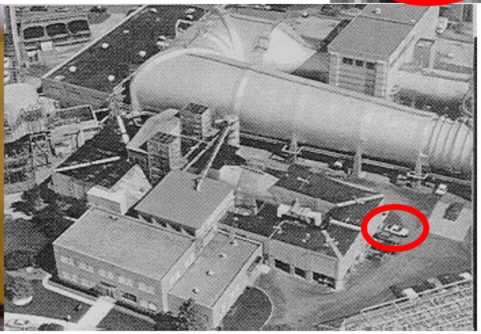

Results and Discussion

Case study(2D ice accretion shapes)

- NASA Icing wind tunnel tests*

IRT case #	308	403	404	405
Airfoil	NACA0012			
$\alpha[\ \ ^\circ]$	4			
$V_\infty[m/s]$	102.8	102.8	102.8	102.8
T_∞[K]	262.04	262.04	256.49	250.3
LWC$[g/m^3]$	1.0	0.55	0.55	0.55
MVD$[\mu m]$	20	20	20	20
Time$[s]$	231	420	420	420
Description	Ice horn case	Mixture condition	Mixture condition	Rime ice
IRT shapes	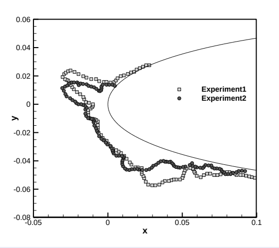	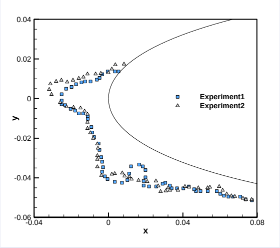	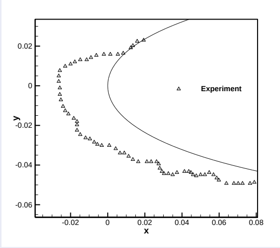	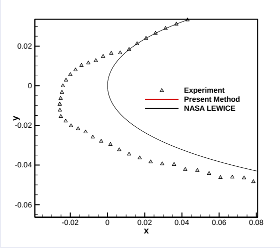

*1) Wright, W. B., "Validation Results for LEWICE 2.0," *NASA Technical Memorandum*, Jan. 1999, pp. 1–679.

Results and Discussion

- Validation results, 4steps